


Full-color, wide field-of-view single-layer waveguide for augmented reality displays

Qian Yang, SID Student Member | Yuqiang Ding, SID Student Member |
Shin-Tson Wu, SID Fellow 

College of Optics and Photonics,
University of Central Florida, Orlando,
Florida, USA

Correspondence

Shin-Tson Wu, College of Optics and
Photonics, University of Central Florida,
Orlando, FL, USA.

Email: swu@creol.ucf.edu

Funding information

Goertek Electronics

Abstract

In the quest for more compact and efficient augmented reality (AR) displays, the standard approach often necessitates the use of multiple layers to facilitate a large full-color field of view (FoV). Here, we delve into the constraints of FoV in single-layer, full-color waveguide-based AR displays, uncovering the critical roles played by the waveguide's refractive index, the exit pupil expansion (EPE) scheme, and the combiner's angular response in dictating these limitations. Through detailed analysis, we introduce an innovative approach, featuring an optimized butterfly EPE scheme coupled with gradient-pitch polarization volume gratings (PVGs). This novel configuration successfully achieves a theoretical diagonal FoV of 54.06° while maintaining a 16:10 aspect ratio.

KEYWORDS

exit pupil expansion, liquid crystal polarization volume grating, waveguide display

1 | INTRODUCTION

Waveguide technologies are becoming increasingly crucial in augmented reality (AR) displays, mainly due to their compact form factor and exit pupil expansion (EPE) capability.^{1,2} Geometric waveguides,³ which employ mirrors and prisms for light coupling, exhibit a minimal wavelength dispersion. This characteristic is particularly advantageous for creating full-color AR displays with a single-layer waveguide. Such a design not only eliminates the misalignment issues⁴ but also simplifies the device assembly process. Nevertheless, a significant challenge arises in the complex fabricating process, mainly due to the requirement for cascading these partially reflective mirrors, which complicates the mass production.⁵

In contrast, diffractive waveguides are significantly impacted by the wavelength dispersion. Even though the grating vectors in all couplers are summed to zero, the total internal reflection (TIR) bandwidth in these

waveguides is still dependent on the wavelength. This results in a wavelength-dependent field of view (FoV), presenting a limitation in single-layer diffractive waveguides.⁶ Therefore, achieving a full-color AR display with a 40° – 70° diagonal FoV (DFoV) typically requires two or three waveguides.⁷ Common types of diffractive waveguide combiners include volume holographic gratings (VHGs) and surface relief gratings (SRGs). VHGs operating in the Bragg regime are known for their large diffraction angles and high diffraction efficiency. However, they usually have limited angular and spectral bandwidths, primarily due to their small index modulation contrast.⁸ On the other hand, SRGs offer a greater design flexibility.⁹ Yet, fabricating certain surface structures, such as those with a large, slanted angle and high aspect ratio, remains challenging.⁵

Recently, polarization volume gratings (PVGs) have emerged as an innovative type of diffractive waveguide combiner.^{10–13} Operating in the Bragg regime, similar to

VHGs, PVGs are distinguished by their composition of liquid crystal. Such a material choice allows for a higher index modulation contrast (0.1–0.3), enabling a broader spectral and angular bandwidth. Their unique response to circularly polarized light, a result of the anisotropic nature of liquid crystals and their helix twist direction, introduces a new dimension to waveguide design. Research by Gu et al. has shown that stacking two PVGs, each responding to an orthogonal polarization but with the same horizontal period, can further increase the angular bandwidth.¹⁴ Additionally, the simple fabrication process of PVGs suggests potential for high yield and cost effectiveness. PVGs also provide the advantage of electrically controlled diffraction efficiency with rapid sub-millisecond response time.¹⁵ The possibility of achieving a full-color AR display with a single PVG waveguide has been explored by Ding et al.⁶ However, their discussion is primarily focused on the 1D EPE scheme.

In this paper, we embark on a comprehensive analysis of the FoV limitations in a single-layer waveguide across various EPE schemes. Our discussion delves into the intricate relationship between the FoV limit and the angular response of the waveguide combiner. We then propose a novel approach, utilizing a gradient-pitch PVG as an input coupler in conjunction with a butterfly EPE

scheme, aiming to reach the theoretical limit of full-color FoV in a single-layer waveguide. Specifically, we introduce an optimized full-color butterfly EPE scheme, which is designed to achieve a 54.06° D FoV with a 16:10 aspect ratio. To validate our approach, we have designed a PVG that meets the requirements of this in-coupler and have thoroughly analyzed the potential FoV crosstalk issues. This analysis is supported by ray-tracing simulations, demonstrating the feasibility and effectiveness of our proposed design.

2 | EPE SCHEMES

Waveguide-based AR displays, while highly valued for their compact form factor and EPE capabilities, confront several challenges, including reduced light efficiency, inadequate color uniformity, and compromised FoV. Besides refractive index, several factors also significantly influence the FoV. In this section, we investigate the factors affecting the FoV of a single-layer waveguide, particularly focusing on how different EPE schemes impact these constraints.

Figure 1A–D illustrates four k -vector diagrams for various EPE schemes.² In these diagrams, the inner circle represents the critical angle of TIR, and the dashed-line

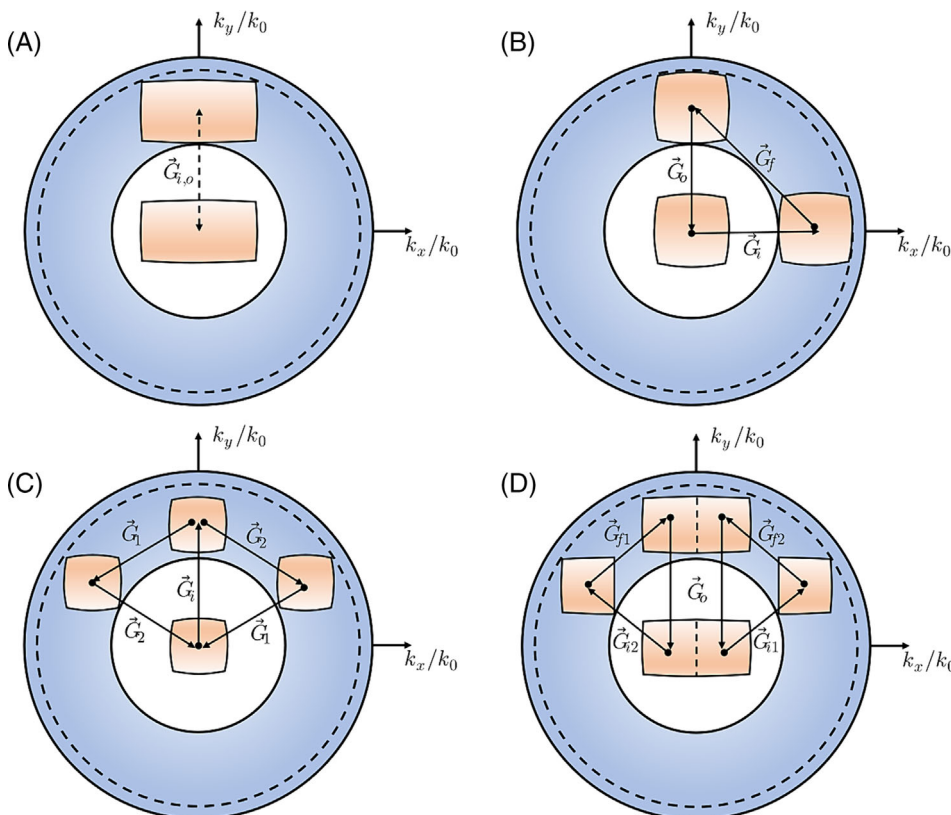


FIGURE 1 Sketch of EPE schemes in k -vector diagrams. (A) 1D. (B) 1D + 1D. (C) 2D. (D) Butterfly.

circle marks the maximum allowable propagation angle. During TIR propagation, the FoV, depicted as an enclosed box, must remain within the annular region between these two circles.

In the 1D EPE scheme, there are only two grating vectors: one for the in-coupler \vec{G}_i and another for the out-coupler \vec{G}_o . Although these vectors have the same magnitude, they are opposite in direction, as shown in Figure 1A. This arrangement allows for the largest possible FoV, but the tradeoff is the increased form factor. In the 1D EPE scheme, since EPE occurs only in one direction, the input coupler for the other direction must be significantly larger to meet the eyebox requirements.⁷ This substantial increase in size is a key reason why the 1D EPE scheme is not commonly adopted in practical applications.

The 1D + 1D EPE scheme offers a proper compromise between FoV and form factor. Illustrated in Figure 1B, this scheme employs three grating vectors: \vec{G}_i for the in-coupler, \vec{G}_f for a secondary grating, and \vec{G}_o for the out-coupler, together forming an enclosed triangle. In this configuration, the FoV is constrained because it has to fit within two distinct positions in the annular region, resulting in a smaller FoV compared to that of the 1D EPE scheme. However, the advantage of this scheme lies in its two-directional EPE, allowing for a smaller in-coupler than what is required in the 1D EPE scheme. This efficient utilization of space, balancing FoV with a

more compact form factor, contributes to the widespread adoption of the 1D + 1D EPE scheme in practical applications.

To further reduce the waveguide's form factor, the 2D EPE scheme has been proposed. This scheme, while similar to the 1D EPE approach in having one in-coupler and one out-coupler, distinguishes itself by utilizing a 2D grating for the out-coupler. The grating vectors, \vec{G}_1 and \vec{G}_2 , enable the 2D grating to simultaneously expand the exit pupil in two directions and out-couple the light. However, despite this advancement, the FoV in the 2D EPE scheme is still subjected to similar limitations as observed in the 1D + 1D EPE scheme. This constraint is illustrated in Figure 1C.

To extend the maximum achievable FoV, the butterfly EPE scheme has been introduced and implemented in Microsoft's HoloLens 2. This innovative approach is depicted in Figure 1D, where the FoV is divided into two separate portions, each managed by its own in-coupler. This design allows each in-coupler to handle a distinct half of the FoV. The scheme then utilizes two folded gratings, each responsible for either the positive or negative part of the FoV. Working in concert, these gratings expand the overall FoV substantially. The two separate FoV segments are then seamlessly integrated, allowing the butterfly EPE scheme to ingeniously bypass FoV limitations while preserving the advantages of 2D EPE.

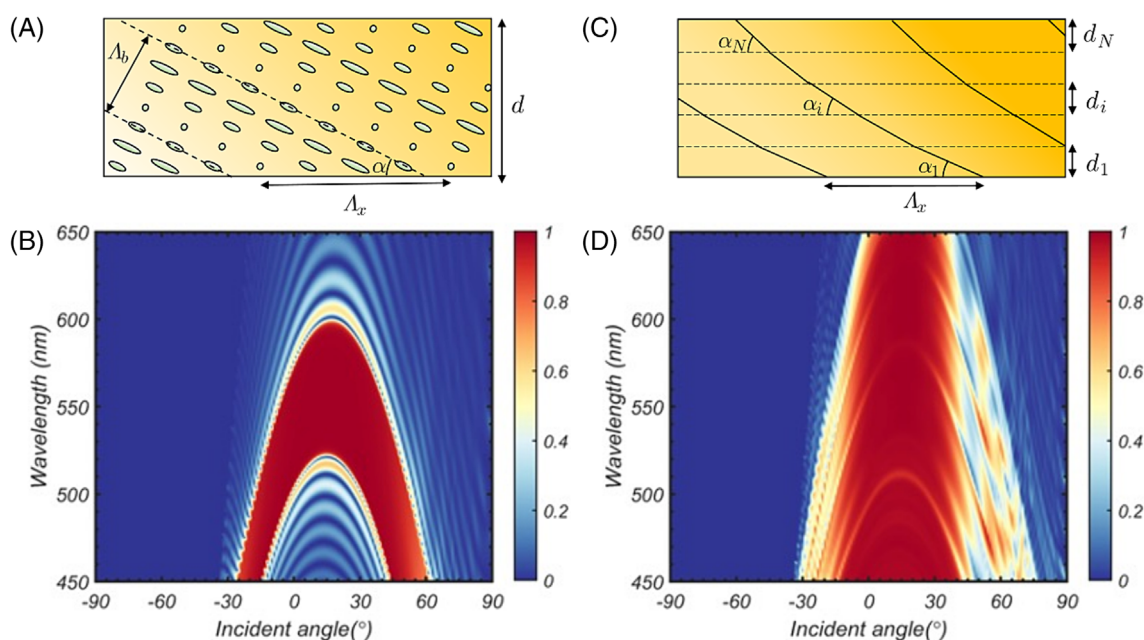


FIGURE 2 (A) The LC orientation of a uniform-pitch PVG. (B) Plot of relation between wavelength-incident angle and diffraction efficiency of a uniform-pitch PVG. (C) The structure of a gradient-pitch PVG. Bragg surfaces in each sublayer are labeled. (D) Plot of relation between wavelength-incident angle and diffraction efficiency of a gradient-pitch PVG.

3 | ASYMMETRIC ANGULAR RESPONSE OF PVG

In AR displays, the FoV is generally expected to be symmetric around 0° . However, Bragg gratings, which are characterized by their high efficiency at a particular diffraction order, exhibit an asymmetric angular response. This asymmetry is also a trait of PVG, which is a specific type of Bragg grating.

The molecular structure of PVG, as shown in Figure 2A, is determined by its horizontal period Λ_x and the slanted angle α , where α represents the tilt of the Bragg plane relative to the horizontal direction. In the spectral and angular space, the high diffraction efficiency band follows a parabola-like trajectory. This is depicted in Figure 2B, which shows the diffraction efficiency for a PVG with $\Lambda_x = 650$ nm and $\alpha = 15.62^\circ$. Here, n_o and n_e are set to be 1.5 and 1.7, respectively, with a PVG thickness of 2 μm . Both the incident and output media have refractive indices of n_{eff} . Notably, while the angular response of the PVG is asymmetric with respect to 0° , it is symmetric around 15° . Generally, its axis of symmetry is given by $\theta = \arcsin(n_{\text{eff}} \sin \alpha)$, which is usually not aligned at 0° . This characteristic presents a limitation in achieving the maximum FoV in waveguide-based AR displays, explaining why PVG does not reach its theoretical limit in the 1D EPE scheme.

Like cholesteric liquid crystal (CLC), the spectral response of PVGs can be enhanced by introducing gradient pitches. In this approach, a gradient-pitch PVG can be divided into N sublayers, as Figure 2C depicts. While each sublayer maintains the same Λ_x , α varies from α_1 to α_N , with each sublayer having a thickness of d_i . One method to achieve this gradient pitch involves doping the CLC mixture with UV dye,¹⁶ followed by exposure to UV light. This process induces a gradient in the chiral dopant concentration. Alternatively, a multiple spin-coating technique¹⁷ can be employed to create gradient-pitch CLC, where each sublayer is given a different chiral dopant concentration. The effectiveness of this method is demonstrated in Figure 2D, which displays the diffraction efficiency of a five-sublayer PVG. Although there is a transitional region close to the substrate where the LC directors transition from a planar alignment to a slanted helical structure, this region is very thin (approximately 50 nm) and therefore has a negligible impact on the simulation of optical properties. This configuration shows a high diffraction efficiency across the entire visible spectrum, from 0° to 30° . In comparison with the PVG presented in Figure 2B, the slanted angles for the five sublayers are set at 13° , 14.9° , 16.1° , 17.1° , and 18° , respectively, with each sublayer being 2 μm thick. Although this method effectively broadens the angular

response of the PVG,^{18,19} it is important to note that the response remains asymmetric due to the inherent nature of PVG. Consequently, despite the broadening, the effective angular bandwidth that can be utilized in AR waveguides is still limited.

4 | OPTIMIZATION OF BUTTERFLY EPE SCHEME

In the butterfly EPE scheme, as previously described, the in-coupler is divided into two segments, each responsible for one half of the FoV. This division effectively relaxes the stringent requirements on the angular response of the in-coupler. As a result, a gradient-pitch PVG, despite exhibiting a single-sided angular response across the visible spectrum, can reach its theoretical full-color FoV limit in this configuration. To achieve this, two gradient-pitch PVGs with opposite polarization response are utilized as in-couplers, with each one addressing a specific segment of the FoV. An important aspect of this setup involves a carefully designed optimization process to determine the appropriate grating vectors. If the grating vector of the in-coupler is chosen to be along the x direction, and the grating vector of the out-coupler to be along the y direction, then the following constraints (Equation 1) should be satisfied on all the available k vectors:

$$\begin{aligned} 1 &\leq (k_x/k_0)^2 + (k_y/k_0 + K_y/k_0)^2 \leq n_g^2 \sin^2 \theta_{\text{max}}, \\ 1 &\leq (k_x/k_0 + K_x/k_0)^2 + (k_y/k_0)^2 \leq n_g^2 \sin^2 \theta_{\text{max}}, \end{aligned} \quad (1)$$

where K_x and K_y are the grating vectors of the in-coupler and out-coupler, respectively. These constraints should be satisfied by the minimum and maximum wavelengths of the full-color spectrum. The objective function is set to maximize the DFoV. To determine the maximum DFoV for each aspect ratio, a nonlinear optimization process is employed. The aspect ratio m is defined as $\tan(\text{HFoV}/2)/\tan(\text{VFoV}/2)$. In this study, we utilize MATLAB's `fmincon` function, a tool for solving constrained nonlinear optimization problems, to find the optimal values. For example, setting $n_g = 2.0$, $\theta_{\text{max}} = 75^\circ$, and $m = 16:10$, we arrive at the results shown in Figure 3A. The maximum FoV is 46.79° horizontally, 30.26° vertically, and 54.06° diagonally, with $\lambda_{\text{min}} = 467.5$ nm and $\lambda_{\text{max}} = 612.5$ nm. As for the grating periods, the required in-coupler has a Λ_x of 334.5 nm, while the out-coupler's Λ_x is 370.7 nm. For the folded grating, Λ_x is 248.3 nm.

The optimization of the gradient-pitch PVG involves adjusting the slanted angle of each sublayer while

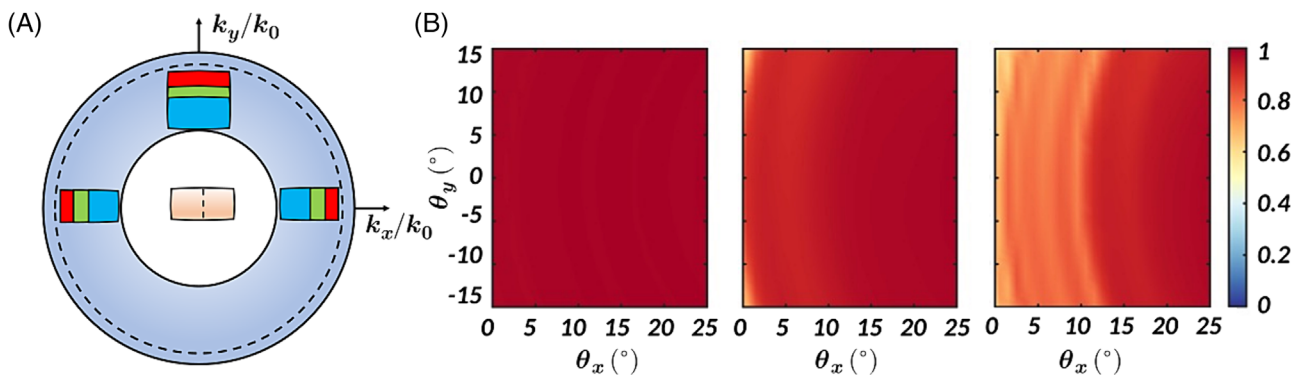


FIGURE 3 (A) The optimized butterfly EPE scheme in a k -vector diagram. (B) Plot of diffraction efficiency versus FoV in air at RGB wavelengths (from left to right: 470, 550, and 610 nm).

keeping their thickness uniform. Through this optimization process, it has been determined that a configuration of six sublayers can meet the in-coupler requirements for the butterfly EPE scheme. The slanted angles for these six sublayers are set at 21.0° , 24.2° , 26.3° , 28.0° , 29.6° , and 31.0° , respectively, with each sublayer having a thickness of $1.67 \mu\text{m}$. Figure 3B illustrates the diffraction efficiency of this optimized PVG at three primary wavelengths: 470, 550, and 610 nm. Notably, the diffraction efficiency spans a range of 0° to 25° horizontally and -15° to 15° vertically across these wavelengths. This comprehensive coverage makes the device suitable for use in the butterfly EPE scheme, realizing the theoretical FoV limit in a single-layer waveguide. Such optimization underscores the potential of gradient-pitch PVG in enhancing the performance of AR displays.

5 | FOV CROSSTALK ANALYSIS

In the optimized butterfly EPE scheme, a potential issue is FoV crosstalk, where the in-coupler designed for one half of the FoV might inadvertently couple light from the other half, leading to a degradation in image quality. To assess and mitigate this issue, we developed a ray-tracing model using LightTools, as depicted in Figure 4A. In this model, the waveguide thickness is set at 0.7 mm. The in-couplers, denoted as I_+ and I_- , are centrally placed in the waveguide, each measuring $1 \text{ mm} \times 1 \text{ mm}$. I_+ handles the left half of the FoV, while I_- manages the right half. Correspondingly, two out-couplers O_+ and O_- are positioned on the left and right sides of the waveguide to couple out their respective halves of the FoV. The out-coupled light is then focused by two ideal lenses LO_\pm ($4 \text{ mm} \times 4 \text{ mm}$) with an 18-mm focal length and captured by plane receivers measuring $7.79 \text{ mm} \times 4.87 \text{ mm}$. Given our focus on crosstalk analysis, rather than conducting a comprehensive eyebox simulation, the

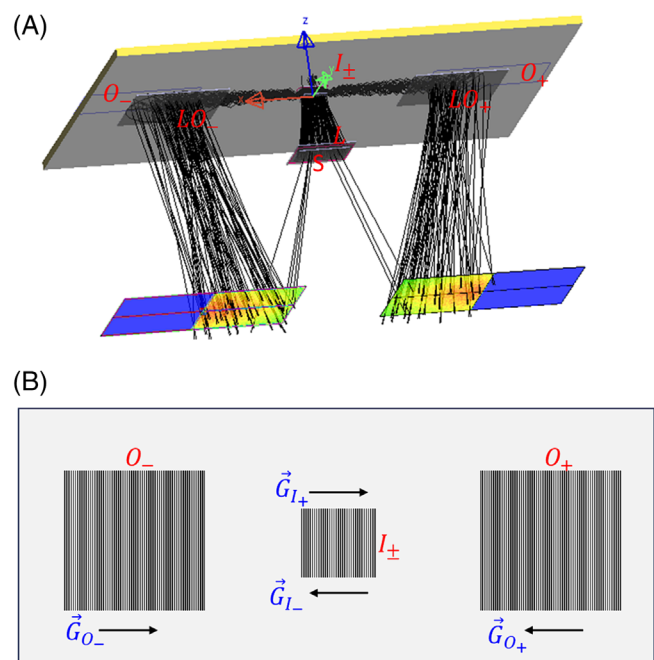


FIGURE 4 Sketch of the ray-tracing model for analyzing FoV crosstalk issue. (A) 3D view. (B) Front view.

out-coupling lens LO_\pm is only positioned at the leading edge of the output coupler, nearest to the input coupler. Additionally, an unpolarized light source (S), sized $4.33 \text{ mm} \times 2.70 \text{ mm}$, is positioned at 5-mm away from the waveguide. An ideal in-coupling lens L (focal length = 5 mm) is laminated to the waveguide. The lens L and input couplers I_\pm have identical dimensions, each measuring 1 mm by 1 mm. To reduce crosstalk between the left and right halves of the FoV, a left-handed circular polarizer is attached to the left half of the display panel, and a right-handed circular polarizer is affixed to the right half. This setup effectively creates two parallel 1D EPE waveguides, as shown in Figure 4B, the front view of the ray-tracing model. By analyzing the light collected

from the two out-couplers, we can evaluate both the in-coupling capability and the extent of FoV crosstalk.

In the ray-tracing model, the optical properties of the two out-couplers are ideally set to achieve 100% diffraction efficiency. For the in-couplers, we use the specifically designed PVG, where I_+ responds to left-handed circular polarization (LCP) and I_- to right-handed circular polarization (RCP). To accurately model the PVG's behavior, we pre-calculate its bi-directional scattering distribution function (BSDF) using a custom rigorous coupled-wave analysis (RCWA) code. The BSDF data generation involves illuminating the PVG with s and p polarization plane waves at each wavelength λ and incident angle (θ, φ) and then recording the reflected and transmitted electric fields across various diffraction orders. The output electric field is also recorded as s and p components, defined in their local coordinate system. Due to the anisotropy of the PVG, the s -polarized incident light can generate diffracted light with both s and p polarizations. For instance, in the BSDF data, a term like r_{sp} represents the p -polarized component of the reflected electric field for the s -polarized incident light.

To streamline the ray-tracing simulation in LightTools, we employ a lookup table method for interpolating the BSDF data. This approach involves storing the BSDF data in a 3D lookup table, with dimensions corresponding to $\lambda, \theta,$ and φ . During the simulation, trilinear interpolation is applied in real-time based on the given wavelength and incident angle. Energy conservation is ensured by adjusting the ray's energy according to the diffraction efficiency. Compared to running RCWA simulations in real-time, this method significantly speeds up the process. We have implemented the lookup table approach in LightTools as a dynamic linked library (DLL), enhancing the efficiency of our ray-tracing simulations.

In our study, we explored two different configurations for arranging the in-couplers in the butterfly EPE scheme, shown in Figure 5A,B. The first option involves stacking the two in-couplers together, as depicted in Figure 5A. The display panel is set to operate at full brightness, without displaying any patterns. Figure 5C shows the spatial luminance collected from the out-coupler O_+ , which corresponds to the left half of the FoV, at wavelengths of 470, 550, and 610 nm, respectively. The

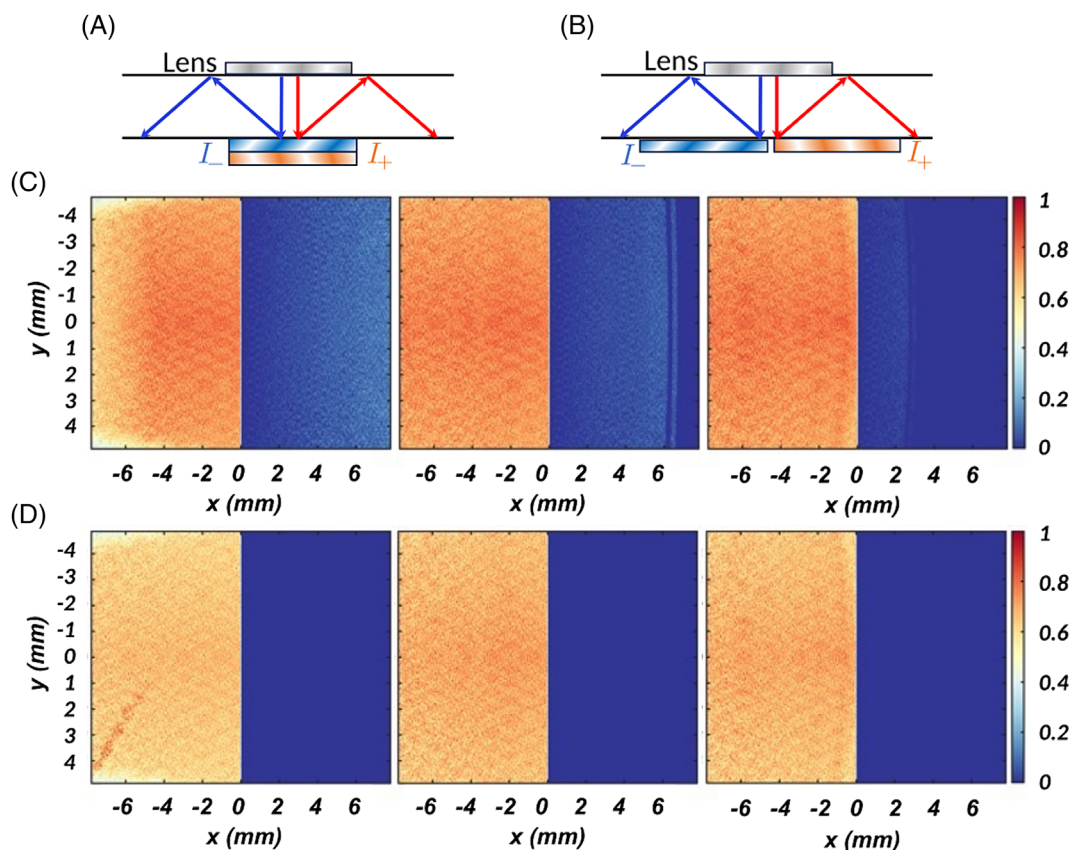


FIGURE 5 Configurations of in-couplers in the butterfly EPE scheme and their associated spatial luminance profiles at RGB wavelengths. (A) In-couplers in a stacked configuration. (B) In-couplers separated by 0.5 mm. The corresponding spatial luminance profiles are shown for (C) the stacked configuration and (D) the 0.5 mm separated configuration, at wavelengths from left to right: blue (470 nm), green (550 nm), and red (610 nm).

spatial luminance profiles reveal the luminance levels across each FoV. While this design effectively covers the left half of the FoV, there is noticeable light leakage into the right half. We define the “leakage ratio” as the ratio of total luminance in the right half of the FoV to that in the left half. At 470, 550, and 610 nm, the leakage ratios are 8%, 4%, and 1%, respectively. The reason is that although the polarization state of the light from the right half FoV is RCP, the light is still partially diffracted by the LCP PVG and coupled out by the out-coupler O_+ . The crosstalk is particularly severe at 470 nm, because the TIR condition is easier to satisfy at a shorter wavelength.

The second configuration, shown in Figure 5B, separates the two in-couplers by a 0.5-mm gap. The spatial luminance from O_+ under this arrangement, indicates a significant reduction in crosstalk, with leakage ratios at all three wavelengths falling below 0.1%, as illustrated by Figure 5D. In this design, it is crucial to align the emission cone of the display panel precisely with the in-coupler positions. For the simulation, we adjusted the aim region of the left and right parts of the light source by 0.75 mm to the left and right, respectively. This adjustment effectively aligns the display panel's emission with the separated in-couplers, resulting in greatly reduced crosstalk.

6 | CONCLUSION

We have conducted a thorough analysis of the FoV limitations in a single-layer, full-color waveguide-based AR display. We discovered that the FoV limit is influenced not only by the refractive index of the waveguide but also significantly by the EPE scheme and the angular response of the waveguide combiner. To mitigate these factors, we proposed to use gradient-pitch PVGs in conjunction with a butterfly EPE scheme. This innovative approach enables the achievement of the theoretical FoV limit. Specifically, we developed an optimized butterfly EPE scheme capable of providing a DFoV of 54.06° with a 16:10 aspect ratio. Additionally, we optimized the in-coupler PVGs for this scheme and constructed a ray-tracing model to assess the system's performance, particularly focusing on mitigating the FoV crosstalk issue.

ACKNOWLEDGMENTS

The authors are indebted to Goertek Electronics for the partial financial support.

ORCID

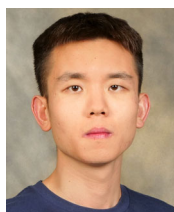
Shin-Tson Wu  <https://orcid.org/0000-0002-0943-0440>

REFERENCES

- Xiong J, Hsiang EL, He Z, Zhan T, Wu ST. Augmented reality and virtual reality displays: emerging technologies and future perspectives. *Light Sci Appl*. 2021;10(1):216. <https://doi.org/10.1038/s41377-021-00658-8>
- Ding Y, Yang Q, Li Y, Yang Z, Wang Z, Liang H, et al. Waveguide-based augmented reality displays: perspectives and challenges. *eLight*. 2023;3(1):24. <https://doi.org/10.1186/s43593-023-00057-z>
- Amitai Y. Extremely compact high-performance HMDs based on substrate-guided optical element. *SID Symp Digest*. 2004; 35(1):310–3. <https://doi.org/10.1889/1.1830976>
- Kress BC, Chatterjee I. Waveguide combiners for mixed reality headsets: a nanophotonics design perspective. *Nanophotonics*. 2021;10(1):41–74.
- Cheng D, Wang Q, Liu Y, Chen H, Ni D, Wang X, et al. Design and manufacture AR head-mounted displays: a review and outlook. *Light Adv Manuf*. 2021;2(3):350–69. <https://doi.org/10.37188/lam.2021.024>
- Ding Y, Li Y, Yang Q, Wu ST. Design optimization of polarization volume gratings for full-color waveguide-based augmented reality displays. *J Soc Inf Disp*. 2023;31(5):380–6. <https://doi.org/10.1002/jsid.1206>
- Kress BC. Optical waveguide combiners for AR headsets: features and limitations. *Proc SPIE*. 2019;11062:110620J.
- Xiong J, Yin K, Li K, Wu ST. Holographic optical elements for augmented reality: principles, present status, and future perspectives. *Adv Photon Res*. 2021;2(1):2000049. <https://doi.org/10.1002/adpr.202000049>
- Kress BC. *Optical architectures for augmented-, virtual-, and mixed reality headsets*. Bellingham: SPIE; 2020.
- Weng Y, Xu D, Zhang Y, Li X, Wu ST. A polarization volume grating with high efficiency and large diffraction angle. *Opt Express*. 2016;24(16):17746–59. <https://doi.org/10.1364/OE.24.017746>
- Weng Y, Zhang Y, Cui J, Liu A, Shen Z, Li X, et al. Liquid-crystal-based polarization volume grating applied for full-color waveguide displays. *Opt Lett*. 2018;43(23):5773–6. <https://doi.org/10.1364/OL.43.005773>
- Yin K, Hsiang EL, Zou J, Li Y, Yang Z, Yang Q, et al. Advanced liquid crystal photonics for augmented reality and virtual reality displays: principles and applications. *Light Sci Appl*. 2022; 11(1):161. <https://doi.org/10.1038/s41377-022-00851-3>
- Weng Y, Zhang Y, Wang W, Gu Y, Wang C, Wei R, et al. High-efficiency and compact two-dimensional exit pupil expansion design for diffractive waveguide based on polarization volume grating. *Opt Express*. 2023;31(4):6601–14. <https://doi.org/10.1364/OE.482447>
- Gu Y, Weng Y, Wei R, Shen Z, Wang C, Zhang L, et al. Holographic waveguide display with large field of view and high light efficiency based on polarized volume holographic grating. *IEEE Photon J*. 2021;14(1):7003707.
- Li Y, Semmen J, Yang Q, Wu ST. Switchable polarization volume gratings for augmented reality waveguide displays. *J Soc Inf Disp*. 2023;31(5):328–35. <https://doi.org/10.1002/jsid.1200>
- Broer DJ, Lub J, Mol GN. Wide-band reflective polarizers from cholesteric polymer networks with a pitch gradient. *Nature*. 1995;378(6556):467–9. <https://doi.org/10.1038/378467a0>

17. Mitov M. Cholesteric liquid crystals with a broad light reflection band. *Adv Mater.* 2012;24(47):6260–76. <https://doi.org/10.1002/adma.201202913>
18. Yin K, Lin HY, Wu ST. Chirped polarization volume grating with ultra-wide angular bandwidth and high efficiency for see-through near-eye displays. *Opt Express.* 2019;27(24):35895–902. <https://doi.org/10.1364/OE.27.035895>
19. Yan X, Wang J, Zhang W, Liu Y, Luo D. Gradient polarization volume grating with wide angular bandwidth for augmented reality. *Opt Express.* 2023;31(21):35282–92. <https://doi.org/10.1364/OE.503493>

AUTHOR BIOGRAPHIES



Qian Yang received his BS degree in Physics from Nanjing University in 2017 and MS degree in Physics from University of Rochester in 2019. He is currently working toward a PhD degree from the College of Optics and Photonics, University of Central

Florida. His current research interests include liquid crystal spatial light modulators for LiDAR applications, planar optics for AR/VR displays, and mini-LED and micro-LED displays.

Yuqiang Ding received his BS degree in Optical Engineering from Shandong University in 2021. He is currently working toward a PhD degree from the

College of Optics and Photonics, University of Central Florida. His current research interests include novel liquid crystal optical elements and optical system design in near-eye displays.

Shin-Tson Wu is a Trustee Chair professor at the College of Optics and Photonics, University of Central Florida (UCF). He is an Academician of Academia Sinica, a Charter Fellow of the National Academy of Inventors, and a Fellow of the IEEE, OSA, SID, and SPIE. He is a recipient of the Optica Edwin H. Land Medal (2022), SPIE Maria Goeppert-Mayer Award (2022), Optica Esther Hoffman Beller Medal (2014), SID Slottow-Owaki Prize (2011), Optica Joseph Fraunhofer Award (2010), SPIE G. G. Stokes Award (2008), and SID Jan Rajchman Prize (2008). In the past, he served as the founding Editor-In-Chief of the *Journal of Display Technology*, Optica publications council chair and board member, and SID honors and awards committee chair.

How to cite this article: Yang Q, Ding Y, Wu S-T. Full-color, wide field-of-view single-layer waveguide for augmented reality displays. *J Soc Inf Display.* 2024. <https://doi.org/10.1002/jsid.1288>